Contents lists available at UGC-CARE

International Journal of Pharmaceutical Sciences and Drug Research

[ISSN: 0975-248X; CODEN (USA): IJPSPP]

journal home page : http://ijpsdr.com/index.php/ijpsdr

Research Article

Design and Synthesis of New Series 6, 7-disubstituted-7H-purine Analogues Induce G2/M cell Cycle Arrest and Apoptosis in Human Breast Cancer SKBR3 cells *via* selective EGFR/HER2 Dual Kinase Inhibition

Chandraprakash Bayya[1*], Sarangapani Manda[2]

[1*]*Department of Pharmaceutical Chemistry, Talla Padmavathi College of Pharmacy, Orus, Kareemabad, Warangal, Telangana, India.*
[2]*Department of Pharmaceutical Chemistry, University College of Pharmaceutical Sciences, Kakatiya University, Warangal, Telangana, India.*

ARTICLE INFO

Article history:
Received: 28 February, 2022
Revised: 23 June, 2022
Accepted: 02 July, 2022
Published: 30 July, 2022

Keywords:
Breast cancer, EGFR, HER2, 6, 7-disubstituted 7H-purine, IC50, lapatinib, etc.

DOI:
10.25004/IJPSDR.2022.140407

ABSTRACT

A unique series of 6, 7-disubstituted 7H-purine analogues were designed with the goal of developing potential EGFR/HER2 dual tyrosine kinase inhibitors to treat human breast cancers. The compounds were rationally developed by replacing the central quinazoline core of lapatinib, an established drug that suppresses both EGFR and HER2, another essential member of this receptor family. Twelve compounds were synthesized by substituting hydrophilic '6-(3-chloro-4-[(substituted pyridin-3-yl) oxy]) anilino' group at 6th position and '(3E)-5-(dimethylamino) pent-3-en-2-ol' side chain at 7th position of purine scaffold which was thought to be considered critical for dual EGFR/HER2 inhibition. The chemical structures of the synthesized compounds were confirmed by 1H, 13C NMR, and HRMS analysis. All these compounds were evaluated for EGFR family tyrosine kinase (EGFR, HER2, HER3, and HER4) *in-vitro* inhibition. The results showed compound 8e as a potent dual EGFR/HER2 inhibitor with IC50 values of 0.021 ± 0.007 μM (EGFR) and 0.019 ± 0.009 μM (HER2), respectively, which were comparable to lapatinib (EGFR: 0.019 ± 0.007; HER2: 0.016 ± 0.003 μM), a positive control. EGFR/HER2 phosphorylation inhibition studies proved potential for 8e in dual kinase inhibition. In support of the dual inhibitory activity against both EGFR and HER2, compound 8e exhibited potent cytotoxic activity against BT-474 and SKBR3 cells, with IC_{50} values of 2.26 ± 0.37 μM (BT-474) and 2.17 ± 0.45 μM (SKBR3), which was comparable to the standard Lapatinib (EGFR: 2.63 ± 0.45 μM; HER2: 1.84 ± 0.39 μM). Additionally, compound 8e caused significant G2/M phase cell cycle arrest, resulting in a fivefold increase in cell number compared to control SKBR3 cells, and potentially induced apoptosis in 79% of these cells, which was comparable to that of lapatinib (83%). These new findings could provide an important basis for further developing compound 8e as a potent EGFR/HER2 dual kinase inhibitor.

INTRODUCTION

The human epidermal growth factor receptor family of receptor tyrosine kinases is composed of EGFR/ErbB-1, HER2/EbB-2, HER3/ ErbB-3, and HER4/ ErbB-4, which have critical roles in cell proliferation, survival, adhesion, migration, and differentiation.[1] Several studies have shown that increased EGFR or other family members overexpression in cancer patients correlates with poor prognosis in several tumor types, including non-small-cell lung cancer (NSCLC), prostate, breast, stomach, colon, and ovarian cancer.[2-6] In particular, elevated levels of EGFR and HER2 gene expression are mainly linked with higher cancer aggressiveness, tumor angiogenesis, postoperative adverse effects, as well as chemotherapy and radiotherapy resistance. Therefore, all existing data support the

***Corresponding Author:** Chandraprakash Bayya

Address: Department of Pharmaceutical Chemistry, Talla Padmavathi College of Pharmacy, Orus, Kareemabad, Warangal, Telangana, India.

Email ✉**:** chandraprakash.bayya@gmail.com

Tel.: 6304811148

Relevant conflicts of interest/financial disclosures: The authors declare that the research was conducted in the absence of any commercial or financial relationships that could be construed as a potential conflict of interest.

rationale for developing antibody-based or small molecule inhibitors as EGFR-targeted therapeutics, and presently, effective blockade of EGFR and HER-2 has been clinically validated in cancer therapy. In 2003 and 2004, the U.S. Food and Drug Administration (USFDA) approved first-generation EGFR tyrosine kinase inhibitors Gefitinib[7] (Iressa™, AstraZeneca) and Erlotinib[8] (Tarceva™, Genentech) (Fig. 1) for EGFR activating mutation-positive NSCLC patients. However, acquired resistance to gefitinib or erlotinib is most common after around 12 months of treatment.[9] The secondary T790M mutation of EGFR is responsible for drug resistance to approved drugs.

In 2007, GlaxoSmithKline got approval for Lapatinib (Tykerb^{TM}) (Fig. 1), an oral dual EGFR/HER2 inhibitor, to treat patients with HER2-over-expressing advanced or metastatic breast cancer. Gefitinib, erlotinib, and lapatinib suppress the EGFR activity by binding competitively to the TK domain's adenosine triphosphate (ATP) binding site.[10] Second-generation of irreversible EGFR inhibitors targeting cys797, such as Afatinib (Gilotrif^{TM}, Boehringer-Ingelheim), Dacomitinib (Vizimpro^{TM}, Pfizer Inc), (Fig. 1), have been designed to overcome EGFRT^{790M} mediated resistance efficiently. Another agent Neratinib (Nerlynx^{TM}, Puma Biotechnology Inc) (Fig 1), was developed to treat HER2 overexpressed breast cancers, and it can be used with or without the combination of chemotherapy. However, the clinical use of new generation irreversible inhibitors is limited due to their poor therapeutic window.[11] The recently approved third-generation drugs, such as osimertinib (Fig. 1), are mutant selective irreversible inhibitors capable of overcoming the previously observed toxicity limitations.[12] By binding covalently to Cys 797, osimertinib targets various sensitizing EGFR mutations, including gatekeeper mutation T790M[13]. Despite encouraging initial outcomes, further resistance develops quickly, with one possible cause being the emergence of new EGFR mutations such as C797S.[14] As a result, continual research efforts in this field are underway with the goal of discovering novel therapeutic candidates to improve patient outcomes.[15-18] Taking into account the intriguing features of lapatinib and similar inhibitors mentioned in the literature[19-25], we have designed and synthesized a new series of twelve 6, 7-disubstituted 7H-purine analogues falling under the general formula shown in Fig. 2. All of them possess the hydrophobic '6-(3-chloro-4-[(substituted pyridin-3-yl) oxy]) anilino' group, which binds with the selectivity pocket and extends into the enzyme's rear pocket, a property considered critical for dual EGFR/HER2 inhibition. Lapatinib's central quinazoline core was replaced with a 7H-purine scaffold (Fig. 2). The hydrophilic solvent exposed '(3E)-5-(dimethylamino) pent-3-en-2-ol' side chain was maintained to optimize the drug-like properties of the designed molecules. The synthesized compounds were evaluated for cytotoxicity to determine their anti-cancer potential against human breast cancer cells. The most active derivatives were then tested for EGFR/HER2 dual inhibitory activity.

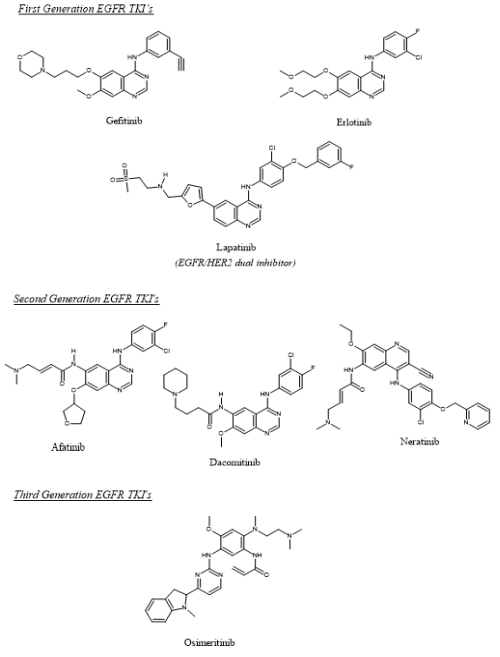

Fig. 1: Approved EGFR and EGFR/HER2 dual inhibitors.

MATERIAL AND METHODS

All chemicals were purchased from Merck as a reagent grade (Darmstadt, Germany). All compounds were purified using column chromatography with silica gel (60-120 mesh) and an eluent solution of hexane and ethyl acetate mixture. Structural confirmations were performed using proton nuclear magnetic resonance (^{1}HNMR) and carbon-13 nuclear magnetic resonance (^{13}CNMR) spectral analysis (Instrument: Bruker Avance II) in DMSO-d_6 at 500 and 125 MHz, respectively. High-resolution mass spectra (HRMS) are recorded on a Bruker Daltronics micro TOF II mass spectrometer. All melting points were uncorrected and measured using Electro-thermal IA 9100 apparatus (Shimadzu, Japan).

General Synthesis

The target compounds 8(a-l) were synthesized as described by T. Ishikawa *et al.*[26] with required modifications.

Synthesis of substituted 3-[(2-chloro-4-nitrophenyl)] pyridine derivatives 3(a-l): substituted pyridine-3-ol's (2a-l, 15.0 mmol) was added to a blend of 2-chloro-1-fluoro-4 nitrobenzene (1, 2.62 g, 15.0 mmol) and potassium carbonate (K_2CO_3) (1.97 g, 15.0 mmol) in DMF (30 mL). After two hours of stirring at 80°C, the mixture was added to 45 mL of water and separated with ethyl acetate (EtOAc). The layer of the organic phase was washed with saturated salt solution (25 mL), vacuum concentrated, and finally dried over anhydrous magnesium sulphate ($MgSO_4$) to yield 3(a-l) as a white solid substance.

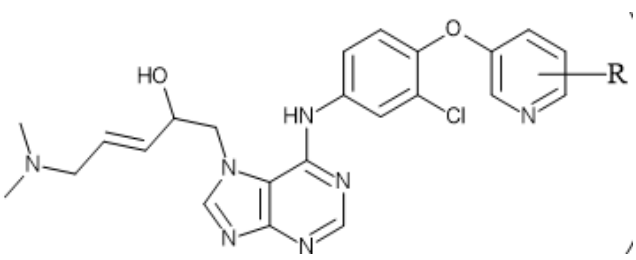

Fig. 2: Optimized 6, 7-disubstituted 7H-Purines

Synthesis of substituted 3-chloro-4-[(pyridin-3-yl)oxy] aniline derivatives 4(a-l): To a solution of 3(a-l) (10 mmol) in EtOAc (50 mL), 5% platinum-carbon (Pt-C) (300 mg) was added, and the reaction contents were agitated for 2.5 hours at room temperature under hydrogen conditions. After removing Pt-C, the extract was concentrated in a vacuum. Purification of the residue using column chromatography (eluent, EtOAc: hexane = 1.5:8.5 to 5:5) yielded 4(a-l) in the form of a white solid.

Synthesis of (3E)-1-(6-chloro-7H-purin-7-yl)-5-(dimethylamino) pent-3-en-2-yl benzoate (6)*:* 1-Iodo-5-(dimethylamino) pent-3-en-2-yl benzoate (1.88 g, 7.01 mmol) was slowly added to a suspension of 6-chloro-7H-purine (**5**, 0.77 g, 5 mmol) and cesium carbonate (1.27 g, 6.58 mmol) in DMF (3.0 mL), and the reaction contents were agitated at normal conditions for 15 hours. Saturated $NaHCO_3$ solution was then added to the resultant mixture, and it was extracted using EtOAc (200 mL x 3). The organic phase was washed with 150 mL of salt solution and dried over $MgSO_4$ before being concentrated in a vacuum. Purification of the residue using column chromatography (eluent, EtOAc: hexane = 7:3 to 5:5) yielded 1.72g (86 %) of 6 as a white solid.

Synthesis of (3E)-1-(6-(4-[-[(pyridin-3-yl)phenoxy]amino)-7H-purin-7-yl)-5-(dimethylamino) pent-3-en-2-yl benzoate derivatives (7a-l)*:* Compounds 4(a-l) (5 mmol) and (3E) -1 (6-chloro-7H-purin-7-yl) -5-(dimethylamino) pent-3-en-2-yl benzoate (6, 5 mmol) were solubilized in 1-methyl-2-pyrrolidone (5.0 mL) and agitated for 3 hours at 100°C. After bringing the vessel contents to normal conditions, it was diluted with 100 mL EtOAc and partitioned with saturated $NaHCO_3$ solution (50 mL). We washed a layer of the organic phase with saturated NaCl solution (50 mL), dried it over $MgSO_4$, and concentrated it in a vacuum. Purification of the residue using column chromatography (eluent, MeOH: EtOAc = 1:4 to 2:8) yielded target compounds 7(a-l) as white crystals. All compounds were successfully synthesized using the same synthetic protocol.

Synthesis of (3E)-5-(dimethylamino)-1-[6-(3-chloro-4-[(pyridin-3-yl)phenoxy]amino)] - 7H-purin-7-yl] pent-3-en-2-ol derivatives (8a-l): The resulting solution of compounds 7a-l in a blend of MeOH (2.5 mL) and THF (2.5 mL) was mixed mechanically at room temperature for 1.5 hours, after which 1N NaOH (0.5 mL) was added. 1N HCl (0.5 mL) was added to the reaction mixture, and the reaction contents were extracted using a mix of EtOAc (3.0 mL) and THF (1.8 mL). a layer of the organic phase was cleansed with saturated salt solution (30 mL), dried over $MgSO_4$, and concentrated in a vacuum. Recrystallization of the residue from EtOAc/diisopropyl ether (2:1) yielded target compounds 8a-l as white crystals.

Anti-cancer evaluation

Kinase inhibitory assays

Selectivity screening of promising compounds against a panel of tyrosine kinases was performed as previously described by B. Sever *et al.*[27], with some changes by utilizing a TK-1 assay kit per the manufacturer's guidelines (Promega Corporation, Madison, WI, USA). Four kinases were used in multipoint dose-response experiments: EGFR, HER2, HER3, and HER4. The kinase and substrate strips were diluted in 45 µL of 5x kinase buffer solution and 7.5 µL of 200 µM ATP, respectively. Kinase reactions were performed using 1 µL of the compound solution at varying concentrations (0.05 µM - 50 µM), 3 µL of kinase working stock, and 3 µL of ATP/substrate working stock. After 1-hour incubation at room 28°C temperature, kinase activity was quantified using the ADP-Glo Kinase Assay (Promega Corporation, Madison, WI, USA). Kinase inhibition was quantified using a luminescence microplate spectrophotometer Infinitive M1000 (Tecan, Groding, Austria). The concentration of the test compounds required to decrease the kinase activity by 50% was determined using ImageJ software and identified as the IC_{50}. In order to monitor and validate the selective inhibitory reaction of EGFR and HER2 with compound 8e, the concentration-dependent study was performed by taking various concentrations at $0.5xIC_{50}$, IC_{50}, and $2xIC_{50}$. This study measures the quantitative behavior of EGFR/HER2 inhibition.

Cellular Cytotoxicity Assays

Human breast adenocarcinoma cells with EGFR and HER2 overexpression (BT-474 and SKBR3), triple-negative breast cancer cell line (HCC38), were provided by the Centre for Cellular and Molecular Biology (CCMB), Hyderabad, India. Cells were cultured in RPMI 1640 medium supplemented with 10% FBS, and Penicillin 100 U/mL and Streptomycin 100 U/mL were added. Cell cultures were maintained in a humidified atmosphere of 5% CO_2 at 37°C. Cells were seeded at respective densities (2.5×10^4/mL) in 96-well plates in a volume of 180 µL per well. After seeding 24 hours, the medium was removed. The test compounds were dissolved in DMSO and diluted with a culture medium to different concentrations (the final concentration of DMSO was 0.1%). Then, 20µL of the test compound solution was added in duplicates, and incubation continued for 48 hours in a humidified atmosphere of 5% CO_2 at 37°C. 20 µL of methylthiazolyldiphenyl-tetrazolium bromide (MTT)

was added to each well after removing the medium and incubated for an additional 3-4 hours. The growth medium was replaced by 150 µL DMSO to solubilize the purple formazan crystals produced, and the absorbance was measured on a microplate reader at 570 nm. The compound IC_{50} values were calculated using Graph Pad Prism 5.0. Data represented as mean ± SD from three independent experiments. Time-dependent cell proliferation inhibition assays against SKBR3 and BT-474 cells were performed at 24, 48, and 72 hours using compound 8e, as the procedure described above.

Apoptotic DNA fragmentation of Compound 8e

We used agarose gel electrophoresis to examine apoptotic DNA fragmentation, which is considered a hallmark of apoptosis, to determine the apoptotic response generated by compound 8e. SKBR3 cells were grown for 48 hours in the absence or addition of 8e at IC_{50} and twice the IC_{50}. Following a conventional process, the genomic DNA was extracted from cells. The DNA samples were run on a 1% agarose gel at 30 V for 6 hours and photographed after being stained with ethidium bromide. Quantification of DNA fragmentation over the treatment of 8e was measured based on the intensity of ethidium bromide-stained onto the genomic DNA of the agarose gel.

Cell Cycle Analysis of Compound 8e

The DNA content of propidium iodide-stained nuclei was analyzed by flow cytometry to determine cancer cell distribution during distinct cell cycle stages, as shown earlier.[28] For 48 hours, the cells were given the IC_{50} of compound 8e or 0.1% DMSO as a control. The cells were then centrifuged after rinsing twice with ice-cold phosphate-buffered saline (PBS). 75% ethanol was added to the cell pellets (-20°C). Following that, cells were stained with the propidium iodide flow cytometry kit (ab139418, Abcam, Cambridge, MA, USA) as directed by the manufacturer. FACS Calibur flow cytometer was used to determine cell cycle distribution (BD Biosciences, San Jose, CA, USA). The CELLQUEST software was used to determine the cell cycle distribution (Becton Dickinson Immunocytometry Systems, San Jose, CA, USA).

Statistical analysis Data are expressed as mean ± SD of the results obtained from at least three independent experiments. Significant differences ($p < 0.05$) between the means of two groups were analyzed by Student's t-test using SPSS 17.0.

RESULTS AND DISCUSSION

Rationale and design

Based on our earlier work with 6,7-disubstituted 7H-purine analogues as EGFR/HER2 dual inhibitors, we planned to develop a new library of analogues with specific dual inhibition and low toxicity by exploring the replacement of 'sulphur' with the 'oxygen' between two aromatic rings of hydrophobic portion' 6-(3-chloro-4-[(substituted pyridin-3-yl) oxy]) anilino moiety' substituted on 6th position of purine scaffold. The rationality behind the design of this series was based on the insight offered by the crystal structure of lapatinib in a complex with EGFR (PDB id.: 1XKK). The inhibitor binds the inactive conformation of the kinase, positioning the 3-fluorobenzyloxy side-chain in a hydrophobic pocket formed next to the ATP binding pocket of the inactive-like kinase by rearrangement of an αC helix (Fig. 3A). In this case, lapatinib is mainly stabilized in the kinase by a hydrogen bond formed at the enzyme hinge between the quinazoline nitrogen N1 and the backbone amide of M793. In contrast, most additional interactions that contribute to the binding of the specific inhibitor are related to the substituents of the quinazoline scaffold.

The crystallographic data show that the 3-fluorobenzyl group is critical for binding to the inactive kinase and, hence, the inhibitor selectivity. It facilitates cation-π and extensive stacking interactions accommodated within the additional pocket aside from the binding site of the nucleotide. Similarly, the methanesulfonyl group is exposed to a considerable extent to the solvent, further stabilizing the bound inhibitor by hydrogen bonds with polar side-chains of the protein surface. The detailed inspection of the interaction mode between lapatinib and EGFR prompted the investigation of an isosteric replacement of the quinazoline core by a ring system with the capacity to accommodate additional hydrogen bonds with the kinase hinge. The imidazole fused pyrimidine scaffold was considered based on the above strategy. The purine scaffold was expected to provide a model for directly comparing the new isosteric heterocyclic system with lapatinib and assess whether an additional hydrogen bonding site could potentially interact with the backbone carbonyl of M793 in a bidentate fashion and further stabilize the inhibitor compared to the original active lead. The substitution of 6-(3-chloro-4-[(substituted pyridin-3-yl) oxy]) anilino moiety on purine scaffold results in binding to the inactive kinase that ultimately results in stabilizing the inactive configuration. The substitution of '(3*E*)-5-(dimethylamino) pent-3-en-2-ol' side-chain simulates the hydrophilic tail of lapatinib by improving the solvent interactions with surface exposure order to optimize the drug-like properties of the molecules. These structural modifications on 7H-purine eventually result in developing a novel class of compounds capable of inhibiting EGFR/HER2.

Chemistry

A novel class of 6,7-disubstituted 7H-purine analogues (8a-i) were synthesized using the process described by Tomoyasu Ishikawa *et al.*[26] to assess the substituent's influence on the terminal pyridine ring. Initially,

2-chloro-1-fluoro-4-nitrobenzene (1) was condensed with several substituted pyridine-3-ol (2a-l) employing dimethylformamide (DMF) solution containing potassium carbonate followed by platinum/carbon driven reduction of the nitro group under hydrogen environment to produce substituted 3-chloro-4-[(pyridin-3-yl)oxy]aniline (4a-l) in excellent yields (67-81%). Further reaction of purified substituted 3-chloro-4-[(pyridin-3-yl)oxy] anilines (4a-l) with 4-(3*E*)-1-(6-chloro-7*H*-purin-7-yl)-5-(dimethylamino)pent-3-en-2-yl benzoate (6) carried out in 1-methyl-2-pyrrolidone (NMP) at 100°C results in dehydrochlorination yielding condensed products 7a-l in moderate to good percentage (39-63%). The hydrolysis of the benzoyl group in the terminal position of 7a-l by 1N aqueous sodium hydroxide (NaOH) resulted in 57-73% yields of the targeted compounds (8a-l) (Fig. 4). The newly synthesized compound structures were in good agreement with their ^{1}H, ^{13}C NMR, and HRMS Spectral investigations. Table 1 lists the structural and physical properties of the generated compounds.

Synthetic scheme

TLC was used to determine the purity of 7H-Purines using a mobile phase of n-hexane: ethyl acetate (7.5:2.5). TLC showed the presence of a single compound. Experimental determination of the melting point of the new derivative was done by open capillary tubes. The structures of all the compounds were confirmed by ^{1}H-NMR, ^{13}C-NMR, and HRMS spectroscopic techniques. The well-known structural characteristics were proposed by ^{1}H-NMR spectroscopy. The proton of aniline group at 6th position of 7H- purine ring appeared in the most downfield region of the spectrum, with a chemical shift of 9.81-10.23 ppm. The hydroxyl group proton of 5-(dimethylamino) pent-3-en group appeared with a chemical shift of 4.99-5.24 ppm. The protons of dimethylamino group at 5th position were appeared in the most upfield region of the spectrum, with a chemical shift of 2.25-2.39 ppm. The large J value (13 Hz)

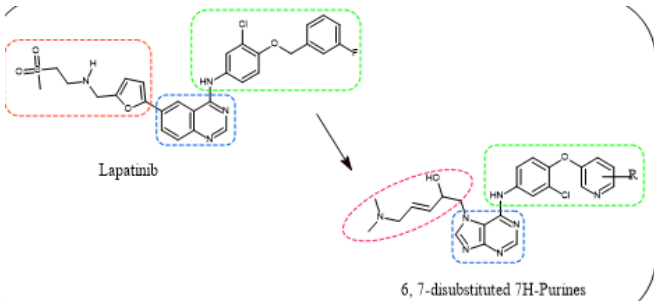

Fig. 3: Rational design of 6,7-disubstituted 7H-Purine analogues based on Lapatinib binding of kinase domain; Greenline molecular portion represents a hydrophobic region that binds to ATP binding site of kinase domain; Blue region of molecule represents central core that stabilizes inactive conformation of kinase upon binding; Red colour region maintains drug-like properties of developed candidates.

Table 1: Yield and melting points of synthesized 6,7-disubstituted 7H-Purines

Entry	*R*	*M.P (oC)*	*Yield (%)*
8a	-H	153.4 -153.9	63.7
8b	-4CH3	161.7 - 162.3	57.6
8c	-5OCH3	163.2 - 163.8	69.2
8d	-5Cl	152.4 - 152.9	72.4
8e	-4Br	156.3 - 157.1	71.8
8f	-5CH3	162.1 - 162.4	58.3
8g	-5CF3	168.3 -168.7	64.9
8h	-4CH3, 6-Br	172.4 - 172.9	61.2
8i	-5CH3, 6-Br	173.6 - 173.8	63.7
8j	-5NH2	167.9 - 168.3	63.1
8k	-6Br	156.2 - 156.5	73.5
8l	-6CF3	169.3 - 169.7	71.6

confirms the trans-type geometrical isomerism (3E) at the double bond. The characteristic carbons of 7H-purine ring appears at 157-154 (down bridgehead carbon), 120-123 (Up bridgehead carbon) 141-153 (ring carbons) in its ^{13}C-NMR spectrum. The signals of double bonded carbons of 5-(dimethylamino) pent-3-en group appeared with a chemical shift of 129-134 ppm in its ^{13}C-NMR spectrum. The carbon signals of dimethylamino group at 5th position were appeared in the most upfield region of the spectrum, with a chemical shift of 39-42 ppm. The HRMS spectra of all 7H-purine compounds represent the base peaks that correspond to $[M+H]^{+}$.

(3E)-5-(dimethylamino)-1-[6-(3-chloro-4-[(pyridin-3-yl) phenoxy]amino)] - 7H-purin-7-yl] pent-3-en-2-ol (8a): ^{1}H-NMR (500 MHz, *DMSO-d6*) δ 9.81 (s, 1H), 8.60 (d, J = 3.49 Hz, 1H), 8.31 (s, 1H), 8.27 (s, 1H), 8.01 (s, 1H), 7.88 (s, 1H), 7.75 (d, J = 8.43 Hz, 1H), 7.43 (dd, J = 7.85, 3.49 Hz, 1H), 7.27 (d, J = 7.85 Hz, 1H), 7.11 (d, J = 8.43 Hz, 1H), 6.14 (dt, J = 14.68, 3.98 Hz, 1H), 5.95 (dd, J = 14.68, 5.68 Hz, 1H), 5.00 (d, J = 5.00 Hz, 1H), 4.51 - 4.44 (d, J = 3.41 Hz, 2H), 4.37 (ddt, J = 5.68, 5.00, 3.41 Hz, 1H), 3.04 - 2.98 (d, J = 3.98 Hz, 2H), 2.25 (s, 6H); ^{13}C NMR (125 MHz, *DMSO-d_6*) δ 157.1, 152.0, 151.9, 151.5, 151.3, 141.9, 140.5, 139.4, 133.0, 131.9, 129.1, 126.4, 126.3, 121.2, 120.5, 118.4, 115.2, 114.2, 68.2, 51.8, 49.7, 39.6 ($2CH_3$); HRMS (ESI) (m/z), of $C_{23}H_{24}ClN_7O_2$ for $[M+H]^{+}$ Calcd: 466.1752; Found: 466.1759.

(3E)-5-(dimethylamino)-1-[6-(3-chloro-4-[(4-methyl pyridin-3-yl) phenoxy]amino)] - 7H-purin-7-yl] pent-3-en-2-ol (8b): ^{1}H-NMR (500 MHz, *DMSO-d6*) δ 10.11 (s, 1H), 8.31 (d, J = 5.64 Hz, 1H), 8.27 (s, 1H), 8.16 (s, 1H), 8.01 (s, 1H), 7.94 (s, 1H), 7.78 (d, J = 8.43 Hz, 1H), 7.35 (d, J = 5.64 Hz, 1H), 7.14 (d, J = 8.43 Hz, 1H), 6.14 (dt, J = 14.68, 3.98 Hz, 1H), 5.95 (dd, J = 14.68, 5.68 Hz, 1H), 5.00 (d, J = 5.00 Hz, 1H), 4.51 - 4.44 (d, J = 3.41 Hz, 2H), 4.37 (ddt, J = 5.68, 5.00, 3.41 Hz, 1H), 3.04 - 2.98 (d, J = 3.98 Hz, 2H), 2.53 (s, 3H), 2.25 (s, 6H); ^{13}C NMR (125 MHz, *DMSO-d_6*) δ 157.1, 151.7, 151.5, 151.3, 150.8, 147.9, 141.9, 139.4, 134.6, 133.0, 132.0, 129.9,

126.4, 123.9, 123.7, 121.1, 118.4, 115.2, 68.2, 58.8, 49.7, 39.6 ($2CH_3$), 15.3; HRMS (ESI) (m/z), of $C_{24}H_{26}ClN_7O_2$ for $[M+H]^+$ Calcd: 480.1909; Found: 480.1913.

(3E)-5-(dimethylamino)-1-[6-(3-chloro-4-[(5-methoxy pyridin-3-yl) phenoxy]amino)] - 7H-purin-7-yl] pent-3-en-2-ol (8c): ^{1}H-NMR (500 MHz, *DMSO-d6*) δ 10.11 (s, 1H), 8.30 (s, 1H), 8.27 (s, 1H), 8.21 (s, H), 8.01 (s, 1H), 7.91 (s, 1H), 7.64 (d, J = 8.43 Hz, 1H), 7.12 (d, J = 8.43 Hz, 1H), 7.01 (s, 1H), 6.14 (dt, J = 14.68, 3.98 Hz, 1H), 5.95 (dd, J = 14.68, 5.68 Hz, 1H), 5.00 (d, J = 5.00 Hz, 1H), 4.51 - 4.44 (d, J = 3.41 Hz, 2H), 4.37 (ddt, J = 5.68, 5.00, 3.41 Hz, 1H), 3.87 (s, 3H), 3.04 -2.98 (d, J = 3.98 Hz, 2H), 2.28 (s, 6H); ^{13}C NMR (125 MHz, *DMSO-d_6*) δ 157.1, 153.9, 152.0, 151.5, 151.3, 148.7, 141.9, 139.4, 133.0, 132.2, 129.1, 128.9, 125.8, 122.8, 121.1, 118.4, 115.5, 101.4, 68.2, 56.1, 52.8, 49.7, 39.6 ($2CH_3$); HRMS (ESI) (m/z), of $C_{24}H_{26}ClN_7O_3$ for $[M+H]^+$ Calcd: 496.1858; Found: 496.1863.

(3E)-5-(dimethylamino)-1-[6-(3-chloro-4-[(5-chloro pyridin-3-yl) phenoxy]amino)] - 7H-purin-7-yl] pent-3-en-2-ol (8d): ^{1}H-NMR (500 MHz, *DMSO-d6*) δ 10.11 (s, 1H), 8.44 (s, 1H), 8.43 (s, 1H), 8.27 (s, 1H), 8.01 (s, 1H), 7.87 (s, 1H), 7.65 (d, J = 8.43 Hz, 1H), 7.44 (s, 1H), 7.14 (d, J = 8.43 Hz, 1H), 6.14 (dt, J = 14.68, 3.98 Hz, 1H), 5.95 (dd, J = 14.68, 5.68 Hz, 1H), 5.00 (d, J = 5.00 Hz, 1H), 4.51 - 4.44 (d, J = 3.41 Hz, 2H), 4.27 (ddt, J = 5.68, 5.00, 3.41 Hz, 1H), 3.04 - 2.98 (d, J = 3.98 Hz, 2H), 2.28 (s, 6H); ^{13}C NMR (125 MHz, *DMSO-d_6*) δ 157.1, 154.8, 151.9, 151.5, 151.3, 145.1, 141.9, 139.4, 133.0, 132.9, 132.1, 129.1, 125.8, 123.7, 121.1, 118.4, 117.2, 115.5, 68.2, 52.8, 49.7, 39.6 ($2CH_3$). HRMS (ESI) (m/z), of $C_{23}H_{23}Cl_2N_7O_2$ for $[M+H]^+$ Calcd: 500.1363; Found: 500.1369.

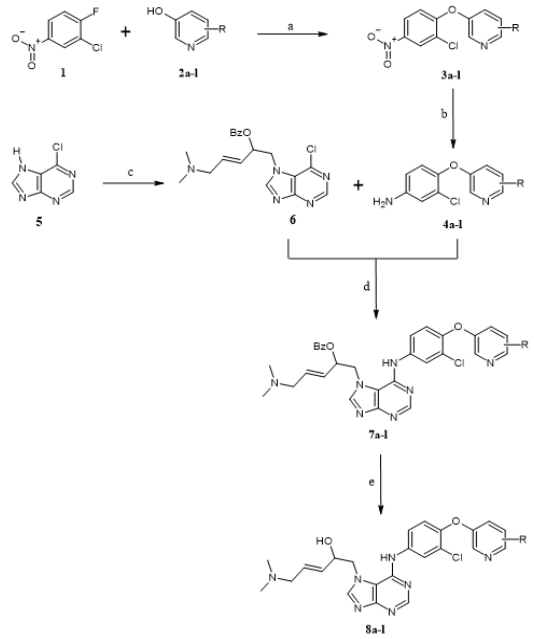

Fig. 4: (a) Potassium carbonate (K2CO3), in Dimethyl formamide (DMF), 80-85°C, 2.5 hours; (b) Pt-C, H2, Ethyl acetate, rt, 2 hour, or CaCl2/Fe in Ethanol, 100°C, 15 hours; (c) (3E)-1-chloro-5-(dimethylamino)pent-3-en-2-yl benzoate, Cs2CO3, DMF, rt, 15 hours; (d) NMP, 100°C, 3 hour, (e) 1N NaOH, MeOH, rt.

(3E)-5-(dimethylamino)-1-[6-(3-chloro-4-[(4-bromo pyridin-3-yl) phenoxy]amino)] - 7H-purin-7-yl] pent-3-en-2-ol (8e): ^{1}H-NMR (500 MHz, *DMSO-d6*) δ 9.81 (s, 1H), 8.60 (s, 1H), 8.41 (s, 1H), 8.27 (s, 1H), 8.01 (s, 1H), 7.81 (s, 1H), 7.78 (d, J = 8.43 Hz, 1H), 7.48 (d, J = 5.64 Hz, 1H), 7.11 (d, J = 8.43 Hz, 1H), 6.14 (dt, J = 14.68, 3.98 Hz, 1H), 5.95 (dd, J = 14.68, 5.68 Hz, 1H), 5.00 (d, J = 5.00 Hz, 1H), 4.51 - 4.45 (d, J = 3.41 Hz, 2H), 4.37 (ddt, J = 5.68, 5.00, 3.41 Hz, 1H), 3.04 -2.98 (d, J = 3.98 Hz, 2H), 2.28 (s, 6H); ^{13}C NMR (125 MHz, *DMSO-d_6*) δ 158.5, 151.7, 151.5, 151.3, 147.8, 141.9, 139.4, 139.0, 133.0, 129.1, 126.3, 125.8, 124.4, 123.4, 121.1, 118.8, 115.4, 115.2, 68.2, 52.8, 49.7, 39.6 ($2CH_3$); HRMS (ESI) (m/z), of $C_{23}H_{23}BrClN_7O_2$ for $[M+H]^+$ Calcd: 544.0857; Found: 544.0863.

(3E)-5-(dimethylamino)-1-[6-(3-chloro-4-[(5-methyl pyridin-3-yl) phenoxy]amino)] - 7H-purin-7-yl] pent-3-en-2-ol (8e):^{1}H-NMR (500 MHz, *DMSO-d6*) δ 10.11 (s, 1H), 8.30 (s, 1H), 8.27 (s, 1H), 8.19 (s, 1H), 8.01 (s, 1H), 7.94 (s, 1H), 7.62 (d, J = 8.43 Hz, 1H), 7.22 (s, 1H), 7.10 (d, J = 8.43 Hz, 1H), 6.14 (dt, J = 14.68, 3.98 Hz, 1H), 5.95 (dd, J = 14.68, 5.68 Hz, 1H), 5.00 (d, J = 5.00 Hz, 1H), 4.51 - 4.44 (d, J = 3.41 Hz, 2H), 4.37 (ddt, J = 5.68, 5.00, 3.41 Hz, 1H), 3.04 - 2.98 (d, J = 3.98 Hz, 2H), 2.32 (s, 3H), 2.25 (s, 6H); ^{13}C NMR (125 MHz, *DMSO-d_6*) δ 157.1, 152.0, 151.9, 151.5, 151.3, 141.9, 140.6, 139.4, 133.0, 132.2, 130.9, 129.1, 126.4, 123.7, 121.1, 118.4, 115.2, 115.0, 68.2, 52.8, 49.7, 39.6 ($2CH_3$), 18.7; HRMS (ESI) (m/z), of $C_{24}H_{26}ClN_7O_2$ for $[M+H]^+$ Calcd: 480.1909; Found: 480.1915.

(3E)-5-(dimethylamino)-1-[6-(3-chloro-4-[(5-trifluoromethyl pyridin-3-yl) phenoxy]amino)] - 7H-purin-7-yl] pent-3-en-2-ol (8g):^{1}H-NMR (500 MHz, *DMSO-d6*) δ 9.87 (s, 1H), 8.58 (s, 1H), 8.31 (s, 1H), 8.27 (s, 1H), 8.01 (s, 1H), 7.80 (s, 1H), 7.54 (d, J = 7.50 Hz, 1H), 7.21 (s, 1H), 7.11 (d, J = 7.50 Hz, 1H), 6.14 (dt, J = 14.68, 3.98 Hz, 1H), 5.95 (dd, J = 14.68, 5.68 Hz, 1H), 5.00 (d, J = 5.00 Hz, 1H), 4.51 - 4.45 (d, J = 3.41 Hz, 2H), 4.37 (ddt, J = 5.68, 5.00, 3.41 Hz, 1H), 3.04 - 2.98 (d, J = 3.48 Hz, 2H), 2.28 (s, 6H); ^{13}C NMR (125 MHz, *DMSO-d_6*) δ 158.5, 151.9, 151.5, 150.6, 148.4, 146.3, 141.9, 139.4, 136.2, 133.0, 129.1, 125.8, 123.1, 123.1, 120.7, 118.4, 118.3 (C), 118.3 (CH), 115.5, 68.2, 52.8, 49.7, 39.6 ($2CH_3$); HRMS (ESI) (m/z), of $C_{24}H_{23}ClF_3N_7O_2$ for $[M+H]^+$ Calcd: 534.1626; Found: 534.1626.

(3E)-5-(dimethylamino)-1-[6-(3-chloro-4-[(4-methyl,6-bromo pyridin-3-yl) phenoxy]amino)] - 7H-purin-7-yl] pent-3-en-2-ol (8h):^{1}H-NMR (500 MHz, *DMSO-d6*) δ 9.81 (s, 1H), 8.27 (s, 1H), 8.09 (s, 1H), 8.01 (s, 1H), 7.87 (s, 1H), 7.65 (d, J = 7.50 Hz, 1H), 7.32 (s, 1H), 7.11 (d, J = 7.50 Hz, 1H), 6.14 (dt, J = 14.68, 3.98 Hz, 1H), 5.95 (dd, J = 14.68, 5.68 Hz, 1H), 5.00 (d, J = 5.00 Hz, 1H), 4.51 - 4.45 (d, J = 3.41 Hz, 2H), 4.37 (ddt, J = 5.68, 5.00, 3.41 Hz, 1H), 3.04 - 2.98 (d, J = 3.48 Hz, 2H), 2.40 (s, 3H), 2.28 (s, 6H); ^{13}C NMR (125 MHz, *DMSO-d_6*) δ158.5, 151.6, 151.5, 151.3, 148.9, 141.9, 139.4, 133.0, 132.3, 129.1, 127.6, 126.0, 125.8, 121.1, 120.7, 118.4, 115.5, 113.6, 68.2, 52.8, 49.7, 39.6 ($2CH_3$), 14.4; HRMS (ESI) (m/z), of $C_{24}H_{25}BrClN_7O_2$ for $[M+H]^+$ Calcd: 558.1014; Found: 558.1018.

(3E)-5-(dimethylamino)-1-[6-(3-chloro-4-[(5-methyl, 6-bromo pyridin-3-yl) phenoxy]amino)] - 7H-purin-7-yl] pent-3-en-2-ol (8i):[1]H-NMR (500 MHz, *DMSO-d6*) δ 9.81 (s, 1H), 8.27 (s, 1H), 8.20 (s, 1H), 8.01 (s, 1H), 7.87 (s, 1H), 7.65 (d, J = 7.50 Hz, 1H), 7.11 (d, J = 7.50 Hz, 1H), 6.98 (s, 1H), 6.14 (dt, J = 14.68, 3.98 Hz, 1H), 5.95 (dd, J = 14.68, 5.68 Hz, 1H), 5.00 (d, J = 5.00 Hz, 1H), 4.51 - 4.45 (d, J = 3.41 Hz, 2H), 4.37 (ddt, J = 5.68, 5.00, 3.41 Hz, 1H), 3.04 - 2.98 (d, J = 3.48 Hz, 2H), 2.28 (s, 6H); ^{13}C NMR (125 MHz, *DMSO-d_6*) δ 158.5, 151.8, 151.5, 151.3, 148.9, 141.9, 139.4, 133.0, 132.5, 129.4, 129.1, 125.8, 121.1, 120.7, 118.4, 118.2, 115.7, 115.5, 68.2, 52.8, 49.7, 39.6 ($2CH_3$), 13.8. HRMS (ESI) (m/z), of $C_{24}H_{25}BrClN_7O_2$ for $[M+H]^+$ Calcd: 558.1014; Found: 558.1019.

(3E)-5-(dimethylamino)-1-[6-(3-chloro-4-[(5-amino pyridin-3-yl) phenoxy]amino)] - 7H-purin-7-yl] pent-3-en-2-ol (8j):[1]H-NMR (500 MHz, *DMSO-d6*) δ 10.11 (s, 1H), 8.34 (s, 1H), 8.30 (s, 1H), 8.27 (s, 1H), 8.01 (s, 1H), 7.87 (s, 1H), 7.54 (d, J = 7.50 Hz, 1H), 7.27 (s, 1H), 7.13 (d, J = 7.50 Hz, 1H), 6.14 (dt, J = 14.68, 3.98 Hz, 1H), 5.95 (dd, J = 14.68, 5.68 Hz, 1H), 5.00 (s,, 2H), 5.00 (d, J = 5.00 Hz, 1H), 4.51 - 4.44 (d, J = 3.41 Hz, 2H), 4.37 (ddt, J = 5.68, 5.00, 3.41 Hz, 1H), 3.04 -2.98 (d, J = 3.48 Hz, 2H), 2.25 (s, 6H); ^{13}C NMR (125 MHz, *DMSO-d_6*) δ 157.1, 153.2, 152.0, 151.5, 151.3, 142.3, 141.9, 139.8, 139.4, 133.0, 132.6, 129.1, 126.4, 123.7, 121.1, 118.4, 115.5, 103.7, 68.2, 58.2, 49.7, 39.6 ($2CH_3$); HRMS (ESI) (m/z), of $C_{23}H_{25}ClN_8O_2$ for $[M+H]^+$ Calcd: 481.1861; Found: 481.1866.

(3E)-5-(dimethylamino)-1-[6-(3-chloro-4-[(6-bromo pyridin-3-yl) phenoxy]amino)] - 7H-purin-7-yl] pent-3-en-2-ol (8k):[1]H-NMR (500 MHz, *DMSO-d6*) δ 9.81 (s, 1H), 8.41 (s, 1H), 8.27 (s, 1H), 8.01 (s, 1H), 7.87 (s, 1H), 7.69 (d, J = 7.50 Hz, 1H), 7.48 (d, J = 8.00 Hz, 1H), 7.28 (d, J = 8.00 Hz, 1H), 7.14 (d, J = 7.50 1H), 6.14 (dt, J = 14.68, 3.98 Hz, 1H), 5.95 (dd, J = 14.68, 5.68 Hz, 1H), 5.00 (d, J = 5.00 Hz, 1H), 4.51 - 4.45 (d, J = 3.41 Hz, 2H), 4.37 (ddt, J = 5.68, 5.00, 3.41 Hz, 1H), 3.04 - 2.98 (d, J = 3.48 Hz, 2H), 2.28 (s, 6H); ^{13}C NMR (125 MHz, *DMSO-d_6*) δ 158.5, 151.9, 151.5, 151.3, 148.3, 141.9, 139.4, 133.0, 129.1, 126.3, 125.8, 123.7, 123.4, 121.1, 118.4, 117.9, 117.5, 115.5, 68.2, 52.8, 49.7, 39.6 ($2CH_3$). HRMS (ESI) (m/z), of $C_{23}H_{23}BrClN_7O_2$ for $[M+H]^+$ Calcd: 544.0857; Found: 544.0865.

(3E)-5-(dimethylamino)-1-[6-(3-chloro-4-[(6-trifluoromethyl pyridin-3-yl) phenoxy]amino)] - 7H-purin-7-yl] pent-3-en-2-ol (8l):[1]H-NMR (500 MHz, *DMSO-d6*) δ 9.87 (s, 1H), 8.52 (s, 1H), 8.27 (s, 1H), 8.01 (s, 1H), 7.87 (s, 1H), 7.57 (d, J = 8.00 Hz, 1H), 7.49 (d, J = 7.50 Hz, 1H), 7.23 (d, J = 8.00 Hz, 1H), 7.13 (d, J = 7.50 Hz, 1H), 6.14 (dt, J = 14.68, 3.98 Hz, 1H), 5.95 (dd, J = 14.68, 5.68 Hz, 1H), 5.00 (d, J = 5.00 Hz, 1H), 4.51 - 4.45 (d, J = 3.41 Hz, 2H), 4.37 (ddt, J = 5.68, 5.00, 3.41 Hz, 1H), 3.04 - 2.98 (d, J = 3.48 Hz, 2H), 2.28 (s, 6H); ^{13}C NMR (125 MHz, *DMSO-d_6*) δ 158.5, 151.9, 151.5, 151.0, 150.6, 141.9, 139.4, 135.9, 133.0, 129.7, 129.1, 125.8, 123.1, 121.1, 120.7 (C), 120.7 (CH), 118.4, 118.3, 115.2, 68.2, 52.8, 49.7, 39.6 ($2CH_3$). HRMS (ESI) (m/z), of $C_{24}H_{23}ClF_3N_7O_2$ for $[M+H]^+$ Calcd: 534.1626; Found: 534.1633.

Anti-cancer Evaluation

Dual kinase inhibition assay

Our principle behind the designed compounds is to improve the EGFR/HER2 dual inhibition and reduce toxicity. Therefore, EGFR and HER2 tyrosine kinase inhibition were used to assess the *in-vitro* enzymatic inhibitory studies that eventually affect tumor inhibitory properties of designed compounds. EGFR and HER2 kinase inhibition assay was performed according to the instructions of the commercial assay developers. As shown in Table 2, three compounds among twelve newly synthesized molecules exhibited moderate to high inhibition activity against EGFR and HER2, which revealed that introducing 4-Bromo, or 5-CF3 or 6-CF3 groups on pyridine ring of 6-anilino moiety on purine scaffold contributed to the activity. Compound 8e of the series exhibited superior suppression of both EGFR/HER2 inhibitory activities among three compounds. Compared to compound 8e, 8g demonstrated considerable dual inhibition, while compound 8l demonstrated moderate inhibition of EGFR activity alone. Substitution of a 4-Br group on a pyridine ring lead to potential dual inhibition, which is evident from the lowest IC_{50} of 0.021 ± 0.007 μM (EGFR) and 0.019 ± 0.009 μM (HER2), which is successfully comparable with that of lapatinib taken as control (EGFR: 0.019 ± 0.007 and HER2: 0.016 ± 0.003) as shown in Fig 5a. Results revealed that no single molecule of the series had demonstrated significant inhibitory activity against other members of the EGFR family, such as HER3 and HER4 (Table 2). EGFR/HER2 dual inhibition of 8e was further confirmed by performing quantitative phosphorylation assays using the same procedure performed above. Based on quantitative research findings, compound 8e suppresses the consumption of ATP by both EGFR and HER2, which falls under the concentration-dependency, resulting in the inhibition of phosphorylation of both kinases (Fig 5b &5c). Comparing compound 8e at twice its IC_{50} concentration with lapatinib at its IC_{50} showed the same effect of EGFR/HER2 dual inhibition. These results demonstrated that the substitution of 6-(3-chloro-4-[(substituted pyridin-3-yl) oxy]) anilino moiety' on 6th position and substitution of '(3E)-5-(dimethylamino) pent-3-en-2-ol' side on 7th position of purine scaffold led to the generation of potent EGFR/HER2 dual inhibitors. In a recent study, purine-based agents were identified that inhibit the protein-protein interaction between β-crystallin and VEGF in triple-negative breast cancers.[29]

In-vitro cytotoxicity studies

The anti-proliferative activity of the new compounds was investigated in the three selected breast cancer cells, SKBR3, BT-474, and HCC38 using lapatinib as the reference compound (Table 3). Six representative concentrations

Table 2: Kinase inhibition of compounds 8a-l.

Entry	*R1*	*Kinase inhibition in IC_{50} (μM)*			
		EGFR	*HER2*	*HER3*	*HER4*
8a	-H	>1	>1	>1	>1
8b	-4CH3	>1	0.952 ± 0.058	>1	>1
8c	-5OCH3	0.825 ± 0.121	0.793 ± 0.103	0.961 ± 0.145	0.988 ± 0.186
8d	-5Cl	0.586 ± 0.095	0.793 ± 0.049	0.512 ± 0.067	0.587 ± 0.054
8e	-4Br	0.021 ± 0.007	0.019 ± 0.009	0.186 ± 0.010	0.199 ± 0.006
8f	-5CH3	0.547 ± 0.096	0.689 ± 0.108	0.628 ± 0.124	0.496 ± 0.089
8g	-5CF3	0.031 ± 0.003	0.028 ± 0.002	0.314 ± 0.008	0.485 ± 0.006
8h	-4CH3, -6Br	0.813 ± 0.159	0.782 ± 0.186	0.855 ± 0.103	0.974 ± 0.147
8i	-5CH3, -6Br	0.785 ± 0.166	0.847 ± 0.192	0.719 ± 0.183	0.856 ± 0.152
8j	- 5NH2	0.498 ± 0.135	0.352 ± 0.124	0.547 ± 0.163	0.688 ± 0.141
8k	-6Br	0.486 ± 0.116	0.509 ± 0.137	0.862 ± 0.195	0.714 ± 0.162
8l	-6CF3	0.039 ± 0.005	0.152 ± 0.003	0.625 ± 0.185	0.596 ± 0.174
Lapatinib	-	0.019 ± 0.007	0.016 ± 0.003	0.218 ±0.087	0.236 ±0.085

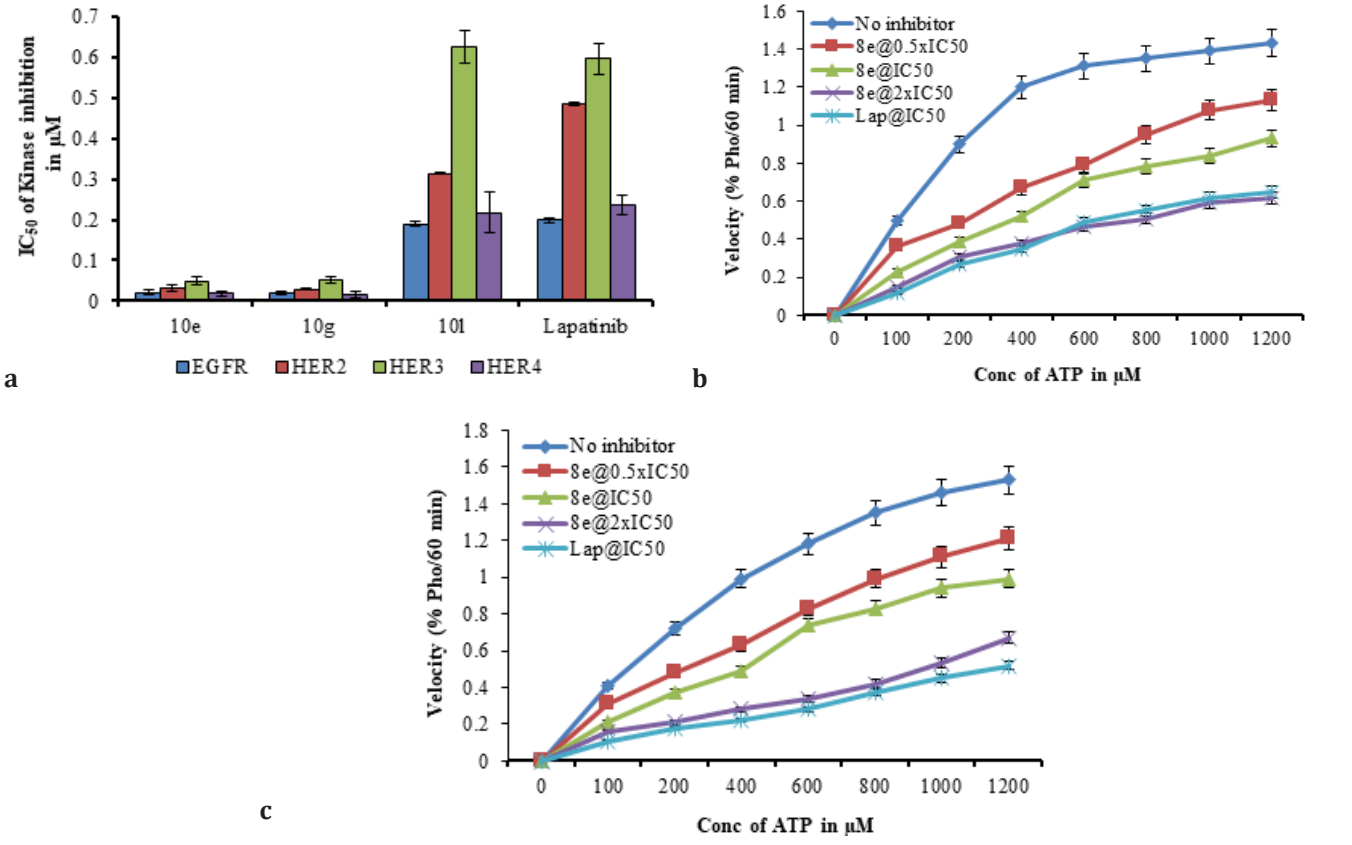

Fig, 5: (a) The kinase inhibition profiles (IC_{50}) of compounds 8e, 8g, and 8l and Lapatinib against EGFR family kinases; Phosphorylation inhibition of EGFR (b) and HER2 (C) over the treatment of compound 8e at 0.5xIC_{50}, IC_{50}, and 2xIC_{50} and Lapatinib at IC_{50}; The data are derived from at least two replicates and presented as mean ± SEM.

ranging from 5 to 50 μM (5, 10, 20, 30, 40, and 50 μM) were used to identify the most potent compounds based on their overall cytotoxicity. Three compounds (8e, 8g, and 8l) possessed high cytotoxicity against both EGFR and HER2 overexpressed BT-474 and SKBR3 cell lines. Compound 8e exhibited a superior cytotoxic effect against both BT-474 and SKBR3, which was evident from the lowest IC_{50} calculated based on non-linear regression analysis (2.26 ± 0.37 μM against BT-474 and 2.17 ± 0.45 μM against SKBR3 cells). Compound 8l and 8g also induced moderate to good

cytotoxicity against both the cells with an IC_{50} of 3.19 ± 0.81 µM (BT-474), 3.68 ± 0.93 µM (SKBR3), and 3.51 ± 0.42 µM (BT-474) 3.87 ± 0.39 µM (SKBR3) respectively (Fig 6a). Interestingly, no single molecule of the series has shown suppression of anti-proliferation in HCC38 cells. Overall, based on the preliminary *in-vitro* cytotoxic evaluation results, compound 8e was selected for further evaluation of dose and time-dependent anti-proliferation against both BT-474 and SKBR3 cells. Results showed a potent dose-dependent and time-independent growth inhibitory activity of compound 8e against BT-474 and SKBR3 cells. In addition, compound 8e showed a higher anti-proliferative effect in SKBR3 cells than BT-474 cells (Fig 6b & c). In light of these results, compound 8e was further evaluated for its ability to determine apoptotic induction.

DNA fragmentation and strand breakage induced by 8e in BT-474 and SKBR3 cells

To elucidate the mode of action of the compound 8e, DNA fragmentation was performed, which is a characteristic feature of the programmed cell death or apoptosis. [30, 31] SKBR3 cells treated with IC_{50} and twice the IC_{50} concentrations of *8e* were harvested after 48 hours, the chromosomal DNA was extracted and used for agarose gel electrophoresis. The result showed fragmentation of DNA leading to a smear in the lanes in which cells were treated with *8e* (Fig. 7). The observed smear resulted from DNA breakage at multiple positions across the chromosomal DNA. The intensity of the smear was maximum at twice the IC_{50} concentration. Quantitative DNA fragmentation was assessed using band intensities, and the results revealed that compound 8e showed the moderate apoptotic effect in 41.62% SKBR3 cells at its $IC_{50,}$ and it potentially induced apoptosis in 79.84 % of cells at twice the IC_{50}, which was comparable with that of lapatinib taken as standard that showed the apoptotic effect in 83.59 % cells.

Table 3: Cellular growth inhibition capabilities (IC_{50} in µM) of novel 6, 7-disubstituted 7H- purines analogues (8a-l) against a panel of breast cancer cells

Entry	*Cell growth inhibition IC_{50}/µMa*		
	SKBR-3	*BT-474*	*HCC38*
8a	12.76 ± 1.89	13.54 ± 1.63	> 15
8b	10.35 ± 2.03	13.11 ± 2.84	> 15
8c	7.61 ± 1.88	9.34 ± 2.19	13.68 ± 2.41
8d	7.33 ± 2.05	6.87 ± 1.36	11.25 ± 1.62
8e	2.26 ± 0.37	2.17 ± 0.45	> 15
8f	13.29 ± 2.75	12.64 ± 2.01	> 15
8g	3.51 ± 0.42	3.87 ± 0.39	> 15
8h	8.21 ± 1.94	8.03 ± 1.11	14.67 ± 2.26
8i	8.92 ± 2.55	9.05 ± 2.23	> 15
8j	11.86 ± 2.17	12.65 ± 1.38	> 15
8k	11.19 ± 1.35	13.64 ± 2.26	11.03 ± 2.49
8l	3.19 ± 0.81	3.68 ± 0.93	14.26 ± 2.04
Lapatinib	2.63 ± 0.45	1.84 ± 0.39	14.95 ± 1.82

[a]The data given are derived from at least two replicates and are presented as mean ± SEM

Compound 8e arrest cell cycle at G2/M Phase

To investigate the cell cycle arrest in support of the cytotoxicity and apoptosis in SKBR3 cells over the treatment of compound 8e, we further analyzed the effects on cell cycle distribution by flow cytometry. The cell cycle distribution analysis revealed that 48 hours of treatment with compound 8e caused a remarkable dose-dependent accumulation of cells in the G2/M phase (Fig. 8). Increasing the concentration from IC_{50} to 2xIC_{50} resulted in a progressive rise in the G2/M-phase cell

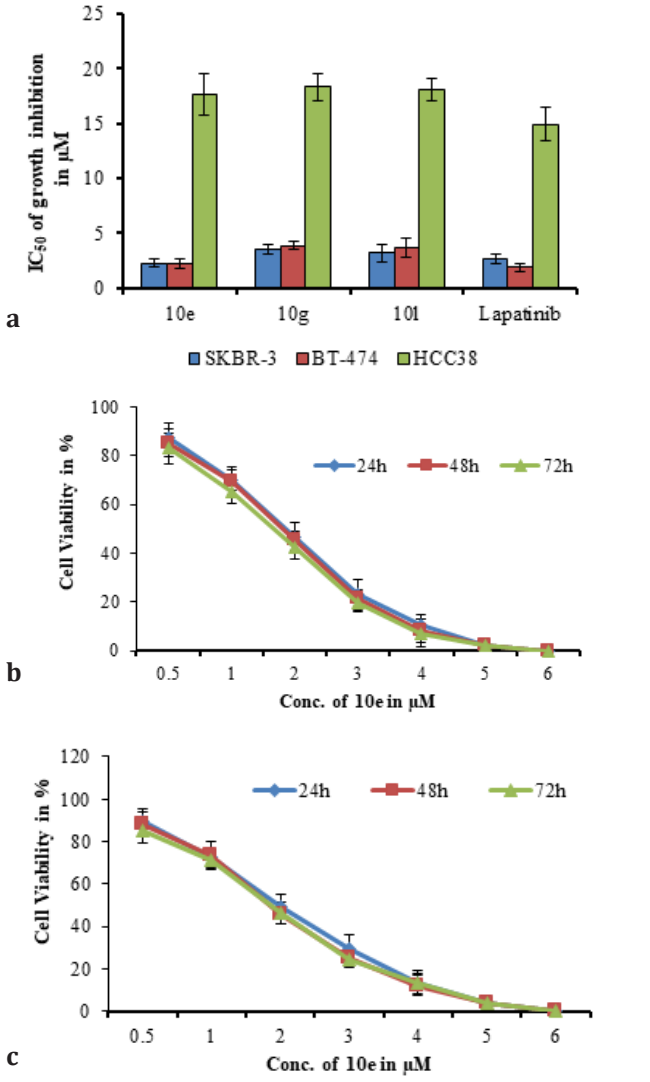

Fig 6: (a) IC_{50} (in µM) of compounds 8e, 8g, and 8l against SKBR-3, BT-474, and HCC38 Cells; Time and concentration dependant cytotoxic effects of compound 8e against SKBR3 (b) and BT-474 (c) cells; The data given are derived from at least two replicates and are presented as mean ± SEM.

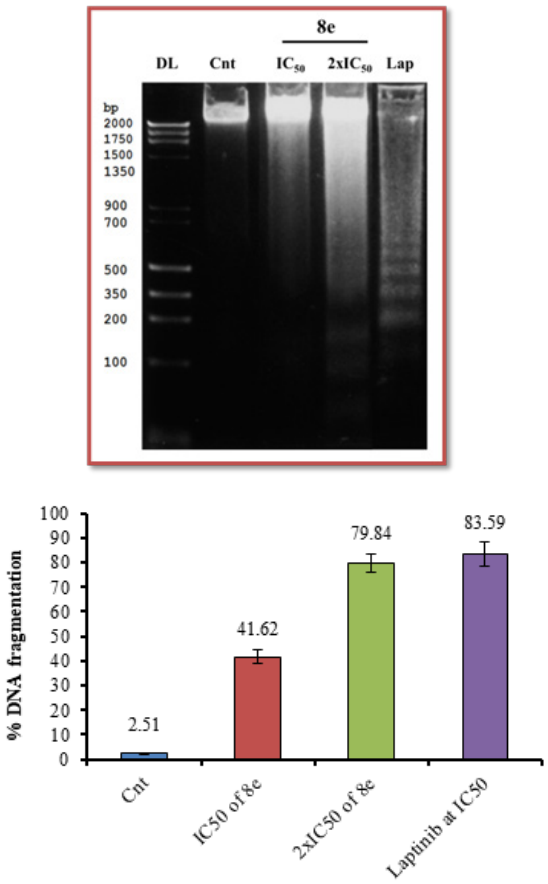

Fig 7: Detection of DNA damage induced by 8e in SKBR3 cells. (a) DNA fragmentation of compound 8e in SKBR3 cells; in this panel, DL represents DNA Ladder; Cnt: Control; (b) quantitative DNA fragmentation of **8e** compared to control in SKBR3 cells; [a]The data given are derived from at least two replicates and are presented as mean ± SEM.

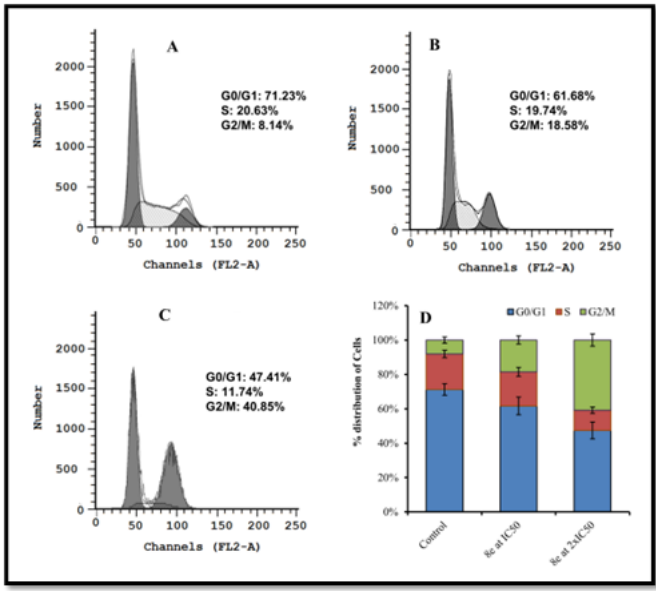

Fig 8: Effects of compound 8e on the induction of G2/M phase arrest in SKBR3 cells, as analyzed by flow cytometry *in-vitro*. Histograms indicate the distribution of the control population of SKBR3 cells (a); 8e at IC_{50} treated cells (b); 8e at $2xIC_{50}$ treated cells (c); stacked column graph representing an overall distribution of cell cycle in test groups at 48 h; The data given are derived from at least two replicates and are presented as mean ± SEM.

population from 18.58 % to 40.85 %, which was significantly higher than the control (8.14 %). Nearly 30% of the S phase cell population was reduced when treated with twice the IC_{50} of 8e, indicating a rise in accumulation of G2/M SKBR3 cells population (Fig. 8). These findings were inconsistent with results reported for 2,6-diamino-substituted purine derivatives in MCF-7 breast and HCT116 colorectal cancer cell lines by Bosco and his colleagues.[32] These results strongly support the potential of compound 8e in inducing cell cycle arrest in HER2-positive breast cancers.

CONCLUSION

We devised and synthesised a new series of 6, 7-disubstituted 7H-purine analogues to enhance kinase inhibitory potential with retain of drug-like features. Based on the principles of rationale design, the hydrophilic '6-(3-chloro-4-[(substituted pyridin-3-yl)oxy]) anilino' group at position 6 and the '(3E)-5-(dimethylamino) pent-3-en-2-ol' at position 7 were considered to be crucial for EGFR and HER2 dual inhibition. Two compounds (8e and 8g) among newly synthesized series demonstrated potential to inhibit EGFR/HER2 dual activity. Compound 8e showed higher kinase suppression efficacy in EGFR/HER2 phosphorylation assays. In addition, compound **8e**, was shown to be a powerful cytotoxic agent in reducing the proliferation of EGFR/HER2 by overexpressed BT-474 and SKBR3 cancer cells. DNA fragmentation studies indicated that compound 8e caused apoptosis in around 80% of SKBR3 cells, similar to standard lapatinib. A fivefold increase in G2/M cell cycle arrest was observed in compound 8e-treated cells at 48 hours after incubation, supporting the apoptosis study. The results showed that the central purine scaffold effectively contributes to anti-cancer efficacy, as evidenced by compound 8e, a potent and promising novel anti-cancer compound with good physicochemical properties and interesting biological activity.

ACKNOWLEDGMENTS

The authors would like to thank the management and principal of Talla Padmavathi College of Pharmacy, Orus, Kareemabad, Warangal, for providing laboratory space and research facilities and their motivation for the successful completion of this work. The authors would also thank the Centre for cellular and molecular biology (CCMB), Tarnaka, Hyderabad, for their continuous support in analyzing the experimental results.

REFERENCES

1. Hynes NE, Lane HA. ERBB receptors and cancer: the complexity of targeted inhibitors. Nature Reviews Cancer. 2005;5:341-354. Available from: doi.org/10.1038/nrc1609.
2. Traxler P. Tyrosine kinases as targets in cancer therapy - successes and failures. Expert Opinion on Therapeutic Targets. 2003;7: 215-234. Available from: doi.org/10.1517/14728222.7.2.215.
3. Sridhar SS, Seymour L, Shepherd FA. Inhibitors of epidermal growth factor receptors: a review of clinical research with a focus on non-small-cell lung cancer. Lancet Oncology. 2003;4: 397-406. Available from: doi.org/10.1016/s1470-2045 (03)01137-9.
4. Vansteenkiste J. Gefitinib (Iressa): a novel treatment for non-small cell lung cancer. Expert Review of Anticancer Therapy. 2004;4: 5-17. Available from: doi.org/10.1586/14737140.4.1.5.
5. Madhusudan S, Ganesan TS. Tyrosine kinase inhibitors in cancer therapy. Clinical Biochemistry. 2004;37: 618-635. Available from: doi.org/10.1016/j.clinbiochem.2004.05.006.
6. Levitzki A. Protein kinase inhibitors as a therapeutic modality. Accounts of chemical research. 2003;36: 462-469. Available from: doi.org/10.1021/ar0201207.
7. Barker AJ, Gibson KH, Grundy W, et al. Studies leading to the identification of ZD1839 (IRESSA): an orally active, selective epidermal growth factor receptor tyrosine kinase inhibitor targeted to the treatment of cancer. Bioorganic & Medicinal Chemistry Letters. 2001;11:1911-1914. Available from: doi.org/10.1016/s0960-894x(01)00344-4.
8. Moyer JD, Barbacci EG, Iwata KK, et al. Induction of apoptosis and cell cycle arrest by CP-358,774, an inhibitor of epidermal growth factor receptor tyrosine kinase. Cancer Research. 1997;57:4838-4848.
9. Pao WMV, Politi KA, Riely GJ, et al. Acquired resistance of lung adenocarcinomas to gefitinib or erlotinib is associated with a second mutation in the EGFR kinase domain. PLOS Medicine. 2005;2:225-235. Available from: doi.org/10.1371/journal.pmed.0020073.
10. Rusnak DW, Lackey K, Affleck K, et al. The effects of the novel, reversible epidermal growth factor receptor/ErbB-2 tyrosine kinase inhibitor, GW2016, on the growth of human normal and tumor-derived cell lines in vitro and in vivo. Molecular Cancer Therapeutics. 2001;1:85-94.
11. Camidge DR, Pao W, Sequist LV. Acquired resistance to TKIs in solid tumours: learning from lung cancer. Nature Reviews Clinical Oncology. 2014;11:473-481. Available from: doi.org/10.1038/nrclinonc.2014.104
12. Yver A. Osimertinib (AZD9291)-a science-driven, collaborative approach to rapid drug design and development. Annals of Oncology. 2016;27:1165-1170. Available from: doi.org/ 10.1093/annonc/mdw129.
13. Cross DA, Ashton SE, Ghiorghiu S, et al. AZD9291, an irreversible EGFR TKI, overcomes T790M mediated resistance to EGFR inhibitors in lung cancer. Cancer discovery. 2014;4:1046-1061. Available from: doi.org/10.1158/2159-8290.CD-14-0337.
14. Minari R, Bordi P, Tiseo M. Third-generation epidermal growth factor receptor tyrosine kinase inhibitors in T790M-positive non-small cell lung cancer: review on emerged mechanisms of resistance. Translational Lung Cancer Research. 2016;5:695-708. Available from: doi.org/10.21037/tlcr.2016.12.02
15. Patel H, Pawara R, Ansari A, Surana S. Recent updates on third-generation EGFR inhibitors and emergence of fourth-generation EGFR inhibitors to combat C797S resistance. European Journal of Medicinal Chemistry. 2017;142:32-47. Available from: doi.org/10.1016/j.ejmech.2017.05.027.
16. Wang S, Song Y, Liu D. EAI045: the fourth-generation EGFR inhibitor overcoming T790M and C797S resistance. Cancer Letters. 2017;385:51-54. Available from: doi.org/10.1016/j.canlet.2016.11.008.
17. Juchum M, Gunther M, Doring E, Sievers-Engler A, Lammerhofer M, Laufer S. Trisubstituted imidazoles with a rigidized hinge binding motif act as single-digit nM inhibitors of clinically relevant EGFR L858R/T790M and L858R/ T790M/C797S mutants: an example of target hopping. Journal of Medicinal Chemistry. 2017;60:4636-4656. Available from: doi.org/10.1021/acs.jmedchem.7b00178.
18. Gunther M, Lategahn J, Juchum M, Doring E, Keul M, Engel J, Tumbrink HL, Rauh D, Laufer S. Trisubstituted pyridinylimidazoles as potent inhibitors of the clinically resistant L858R/T790M/C797S EGFR mutant: targeting of both hydrophobic regions and the phosphate binding site. Journal of Medicinal Chemistry. 2017;60:5613-5637. Available from: doi.org/10.1021/acs.jmedchem.7b00316.
19. Bugge S, Kaspersen SJ, Larsen S, Nonstad U, Bjorkoy G, Sundby E, Hoff BH. Structure-activity study leading to identification of a highly active thienopyrimidine based EGFR inhibitor. European Journal of Medicinal Chemistry. 2014;75:354-374. Available from: doi.org/10.1016/j.ejmech.2014.01.042.
20. Buskes MJ, Clements M, Bachovchin KA, Jalani HB, Leonard A, et al. Structure-Bioactivity Relationships of Lapatinib Derived Analogs against Schistosoma mansoni. ACS Medicinal Chemistry Letters. 2020;10;11(3):258-265. Available from: doi.org/10.1021/acsmedchemlett.9b00455.
21. Lin J, Shen W, Xue J, Sun J, Zhang X, Zhang C. Novel oxazolo[4,5-g] quinazolin-2(1H)-ones: dual inhibitors of EGFR and Src protein tyrosine kinases. European Journal of Medicinal Chemistry. 2012;55;39-48. Available from: doi.org/10.1016/j.ejmech.2012.06.055.
22. Petrov KG, Zhang YM, Carter M, et al. Optimization and SAR for dual ErbB-1/ErbB-2 tyrosine kinase inhibition in the 6-furanylquinazoline series. Bioorganic & Medicinal Chemistry Letters. 2006;16:4686-4691. Available from: doi.org/10.1016/j.bmcl.2006.05.090
23. Olszewska P, Cal D, Zagórski P, Mikiciuk-Olasik E. A novel trifluoromethyl 2-phosphonopyrrole analogue inhibits human cancer cell migration and growth by cell cycle arrest at G1 phase and apoptosis. European journal of pharmacology. 2020;15;871:172943. Available from: doi.org/10.1016/j.ejphar.2020.172943.
24. Jin H, Wu BX, Zheng Q, Hu CH, Tang XZ, Zhang W, Rao GW. Design, synthesis, biological evaluation and docking study of novel quinazoline derivatives as EGFR-TK inhibitors. Future Medicinal Chemistry. 2021;13(7):601-612. Available from: doi.org/10.4155/fmc-2020-0015.
25. Farghaly TA, Abbas EMH, Al-Soliemy AM, Sabour R, Shaaban MR. Novel sulfonyl thiazolyl-hydrazone derivatives as EGFR inhibitors: Design, synthesis, biological evaluation and molecular docking studies. Bioorganic Chemistry. 2022;121:105684. Available from: doi.org/10.1016/j.bioorg.2022.105684.
26. Ishikawa, T, Seto M, Banno H, Kawakita Y, Oorui M, Taniguchi T. Design and Synthesis of Novel Human Epidermal Growth Factor Receptor 2 (HER2)/Epidermal Growth Factor Receptor (EGFR) Dual Inhibitors Bearing a Pyrrolo [3,2-d] pyrimidine Scaffold. Journal of Medicinal Chemistry. 2011;54(23):8030-8050. Available from: doi.org/10.1021/jm2008634.
27. Sever B, Altıntop MD, Radwan MO, Ozdemir A, Otsuka M, Fujita M, Ciftci HI. Design, synthesis and biological evaluation of a new

series of thiazolyl-pyrazolines as dual EGFR and HER2 inhibitors. European Journal of Medicinal Chemistry. 2019;182:1116-1128. Available from: doi.org/10.1016/j.ejmech.2019.111648.

28. Abaza MS, Bahman AM, Al-Attiyah RJ. Valproic acid, an anti-epileptic drug and a histone deacetylase inhibitor, in combination with proteasome inhibitors, exerts anti-proliferative, pro-apoptotic and chemosensitizing effects in human colorectal cancer cells: Underlying molecular mechanisms. International Journal of Molecular Medicine. 2014;34:513-532. Available from: doi.org/10.3892/ijmm.2014.1795.
29. Fosu-Mensah NA, Jiang W, Brancale A, Jun C, Westwell AD. The discovery of purine-based agents targeting triple-negative breast cancer and the αB-crystallin/VEGF protein-protein interaction. Medicinal Chemistry Research. 2019;28:182-202. Available from: doi.org/10.1007/s00044-018-2275-9.
30. D'Arcy MS. Cell death: a review of the major forms of apoptosis, necrosis and autophagy. Cell Biology International. 2019;43(6):582-592. Available from: doi.org/10.1002/cbin.11137.
31. Hu XM, Li ZX, Lin RH, Shan JQ, Yu QW, Wang RX, Liao LS, Yan WT, Wang Z, Shang L, Huang Y, Zhang Q, Xiong K. Guidelines for Regulated Cell Death Assays: A Systematic Summary, A Categorical Comparison, A Prospective. Frontiers in Cell and Developmental Biology. 2021;4(9):634-690. Available from: doi.org/10.3389/fcell.2021.634690.
32. Bosco B, Defant A, Messina A, Incitti T, Sighel D, Bozza A, Ciribilli Y, Inga A, Casarosa S, Mancini I. Synthesis of 2,6-Diamino-Substituted Purine Derivatives and Evaluation of Cell Cycle Arrest in Breast and Colorectal Cancer Cells. Molecules. 2018 10;23(8):1996. Available from: doi.org/10.3390/molecules23081996.

HOW TO CITE THIS ARTICLE: Bayya C, Manda S. Design and synthesis of New Series 6, 7-disubstituted-7H-purine Analogues Induce G2/M cell Cycle Arrest and Apoptosis in Human Breast Cancer SKBR3 cells *via* selective EGFR/HER2 dual Kinase Inhibition. Int. J. Pharm. Sci. Drug Res. 2022;14(4):402-413. **DOI:** 10.25004/IJPSDR.2022.140407